OPEN ACCESS
International Journal of Innovations in Science & Technology

UAV-Based Flood Mapping and Damage Assessment in Harnai Khawar, Swat, Khyber Pakhtunkhwa, Pakistan

Iqra Hameed[1], Rabia Qadir[1], Amir Ali[1], Muhammad Sohail[2], Saif Ullah Akhter[3]
[1]Institute of Space Science, University of the Punjab, Lahore
[2]Department of Geography, Government Graduate College of Science, Wahdat Road, Lahore
[3]Department of Geography, Government Associate College, Eminabad, Gujranwala
*Correspondence: geospatialresearch47@gmail.com

Citation | Hameed. I, Qadir. R, Ali. A, Sohail. M, Akhter. S. U, "UAV-Based Flood Mapping and Damage Assessment in Harnai Khawar, Swat, Khyber Pakhtunkhwa, Pakistan", IJIST, Vol. 07 Issue. 04 pp 2679-2690, November 2025
DOI: https://doi.org/10.33411/IJIST/1609
Received | October 02, 2025 **Revised |** October 17, 2025 **Accepted |** October 23, 2025 **Published |** November 04, 2025.

Floods is among the most destructive hydrological hazards in Pakistan, particularly across the steep, data‑sparse basins of Khyber Pakhtunkhwa (KPK). The 2022 monsoon produced catastrophic damage in the Swat Valley, disrupting transport, irrigation, and housing. This article demonstrates an Unmanned Aerial Vehicle (UAV) workflow for rapid, high‑resolution flood mapping, damage quantification, and risk zonation in the Barwai Khwar sub‑watershed of the Swat River Basin. Pre‑event context was assembled from Google Earth Pro imagery (12 June 2022), and post‑event aerial surveys were flown using a DJI Phantom 4 Pro (v2.0) with GNSS‑supported Ground Control Points (GCPs). Imagery was processed in Agi soft Meta shape to generate Ortho mosaics and surface products, then analyzed in a GIS to delineate inundation, channel widening, structural damage, and agricultural losses. The floodplain width locally expanded from approximately 7 m to 76 m; damaged linear infrastructure includes ~2.18 km of retaining walls and 39 m of bridges. Surface impacts include ~6,271 m² of residential area and ~22.56 ha of cropland affected. The approach provided near‑centimeter spatial detail, enabling precise polygonal accounting for recovery planning and identification of high‑risk margins where unprotected construction coincides with steep banks and tight meanders. Findings confirm the value of UAV photogrammetry as a fast, replicable, and cost‑effective complement to satellite‑based disaster assessment in Pakistan's mountain valleys, supporting preparedness, reconstruction, and resilient land‑use decisions.

Keywords: Flood Assessment; UAV Imagery; Swat Basin; Aerial Photogrammetry; GNSS; GIS; Disaster Management

Introduction:

Flooding ranks among the most devastating natural hazards, leading to significant loss of life, property damage, and environmental disruption worldwide. In Pakistan, irregular monsoon rainfall, deforestation, and rapid urban expansion within floodplains have intensified flood impacts over the past decades [1][2]. The Swat River Basin in Khyber Pakhtunkhwa (KPK) is among the most vulnerable regions, where heavy rainfall and steep slopes generate flash floods that devastate agricultural land, infrastructure, and local livelihoods [3]. Conventional ground surveys are often time-consuming and difficult to conduct in mountainous terrain, limiting their usefulness for timely disaster assessment. Recent advances in remote sensing, particularly high-resolution aerial imagery from Unmanned Aerial Vehicles (UAVs), have transformed flood assessment by providing precise, near-real-time data on damage extent and landscape change [4][5]. Integration of UAV imagery with Geographic Information System (GIS) platforms enables accurate mapping of inundation, erosion, and infrastructure damage, supporting evidence-based recovery planning [4]. Numerous studies worldwide have demonstrated the effectiveness of UAVs in post-disaster evaluation. For example, Zawadzka et al. (2021) [6] applied object-oriented classification to UAV imagery to identify flood-induced damage in residential areas, while Hashemi-Beni et al. (2018) [7] assessed the utility of UAV-derived DEMs for mapping flood extents in North Carolina, USA. In data-scarce regions, Wouters et al. (2021) [8] combined UAV segmentation with machine learning to estimate flood impacts in southern Malawi. These examples confirm that UAV-based photogrammetry offers a rapid, cost-effective, and high-resolution method for flood damage assessment, particularly where traditional satellite or field surveys face limitations. However, in Pakistan, especially within steep and remote basins such as Swat, UAV-based flood mapping remains underexplored. The Barwai Khwar sub-watershed, therefore, provides an opportunity to evaluate the precision and applicability of UAV photogrammetry for localized disaster assessment. This study presents one of the first comprehensive UAV-based flood assessments conducted in northern Pakistan. Unlike conventional post-disaster surveys, it integrates centimeter-level UAV orthomosaics with GIS analytics to develop a spatially detailed inventory of flood-induced damage. The proposed workflow enables reproducible, high-accuracy mapping suitable for emergency response, rehabilitation, and future resilience planning in mountainous environments.

Objectives:

This study aims to develop a high-resolution, UAV GIS-based workflow for rapid flood damage assessment in Harnai Khawar, Swat, Khyber Pakhtunkhwa. The main objectives are:

To quantify flood-induced damage to built-up areas, retaining walls, agricultural land, and bridges through pre- and post-event UAV imagery comparison and GIS-based spatial analysis.

To evaluate geomorphic and infrastructural changes in the Harnai Khawar sub-basin, providing actionable information for post-flood rehabilitation and resilience planning. This research introduces one of the first UAV-based, centimeter-scale flood assessment frameworks applied in a mountainous valley of northern Pakistan. The integration of high-overlap UAV orthomosaics with geospatial analytics allows accurate measurement of channel widening, structural losses, and land-cover changes in complex topography where conventional satellite or field surveys are limited. The proposed approach demonstrates a replicable, cost-effective method for localized disaster assessment and climate resilience mapping in data-scarce mountain environments.

Material and Methods:

Study Area:

Harnai Khawar (35° 11' 45" N, 72° 33' 22" E), a region located in the picturesque Swat valley of Khyber Pakhtunkhwa (KPK), Pakistan, has been a historically significant area with diverse landscapes and cultural heritage. However, similar to many areas in Khyber Pakhtunkhwa (KPK), Harnai Khawar is highly susceptible to multiple natural hazards such as floods, landslides, and earthquakes. Among these, floods stand out as the most frequent and destructive, posing severe risks to human lives, infrastructure, and the surrounding environment. This case study focuses on Harnai Khawar to examine the flood-related challenges confronting the area and to evaluate the potential of high-resolution aerial imagery for effective flood damage assessment and disaster management. Harnai Khawar is situated in the upper reaches of the Swat Valley, approximately 30 kilometers northeast of the district capital, Mingora. It is surrounded by majestic mountains, including the Hindukush and Karakoram ranges, making the region susceptible to rapid runoff during heavy rainfall events. The area is characterized by its fertile plains, which have supported agricultural activities for generations, forming the backbone of the local economy. Numerous small streams and rivulets traverse the region, eventually converging into the Swat River, which flows through the heart of the valley. The proximity of Harnai Khawar to the river and its tributaries exposes it to the risk of frequent floods, particularly during the monsoon season. During monsoons, the region experiences intense and prolonged rainfall, leading to a significant increase in water levels in the streams and the Swat River [9]. The mountainous terrain and the impermeable nature of the soil in some areas further contribute to rapid runoff, exacerbating the flood risk. The combination of heavy rainfall, steep topography, and inadequate drainage systems can result in flash floods and inundation of low-lying areas [10]. Such floods can have severe impacts on the community, causing extensive damage to crops, infrastructure, and property, while also posing significant risks to human lives [11].

Mitigating the effects of these frequent floods requires local authorities and communities to establish and enforce effective flood preparedness and response measures. These may include early warning systems, improved drainage infrastructure, land-use planning, and awareness campaigns to ensure the safety and resilience of Harnai Khawar and its inhabitants during monsoon seasons.

Approach and Methodology:

The workflow integrated pre- and post-flood data collection, UAV-based photogrammetry, image processing, and GIS analysis to spatially map the impacts of the 2022 flood in Harnai Khawar, Swat. The approach enabled comparison between pre-flood conditions and post-flood landscape transformation (Figure 1).

Data Collection:

Pre-Flood Dataset:

Pre-flood conditions were established using high-resolution satellite imagery from Google Earth Pro (12 June 2022). These images provided a reliable baseline of land cover, agricultural fields, and infrastructure before inundation. Although Google Earth imagery offers moderate spatial resolution compared to UAV data, it remains a valuable open-source resource for pre-event reference in regions where dedicated aerial or satellite acquisitions are unavailable. The dataset was georeferenced and corrected in ArcGIS Pro to ensure accurate spatial alignment with the UAV-derived orthomosaics.

Post-Flood UAV Survey:

Post-event mapping was performed using a DJI Phantom 4 Pro (v2.0) UAV equipped with a 20 MP 1-inch CMOS sensor and Global Navigation Satellite System GNSS-based autopilot. The quadcopter captured between 150 and 170 overlapping images per flight at an altitude of 150 meters, with 80% forward and 70% side overlap. Ground Control Points

(GCPs) were surveyed using Global Navigation Satellite System (GNSS) to ensure precise spatial accuracy. Equipped with obstacle-avoidance and stability features, the UAV enabled safe and detailed mapping of the flood-affected valley. The post-flood aerial survey comprised four separate flight missions conducted over two consecutive days in early September 2022. Each flight covered approximately 0.9 to 1.2 km² of the valley floor with an average duration of 18 to 22 minutes, corresponding to a single battery cycle of the DJI Phantom 4 Pro v2.0. The UAV was operated between 10:00 a.m. and 3:00 p.m. under clear to partly cloudy conditions, with average surface temperatures of 28 to 30 °C, wind speeds below 4 m s^{-1}, and no measurable precipitation. Low wind velocity and stable illumination ensured optimal overlap consistency and minimized motion blur in captured images. Weather information was verified using the Pakistan Meteorological Department (PMD) station data for Mingora, Swat, confirming calm conditions during both survey days.

The combination of short flight intervals, stable atmospheric conditions, and high image overlap produced sharp, distortion-free photographs suitable for precise orthomosaic generation in Agisoft Metashape.

Image Processing and Rectification:

The collected images were processed in Agisoft Metashape Professional following a standard photogrammetric workflow. The procedure involved image alignment and dense point-cloud generation, followed by mesh reconstruction and orthomosaic creation. Manual masking was applied to remove background noise, and final orthorectification was performed using interior and exterior orientation parameters with GCP-based correction to ensure geometric accuracy. Each image was rectified to an orthogonal projection to maintain uniform scale and geometric accuracy. The final orthomosaic was exported in GeoTIFF format for GIS analysis.

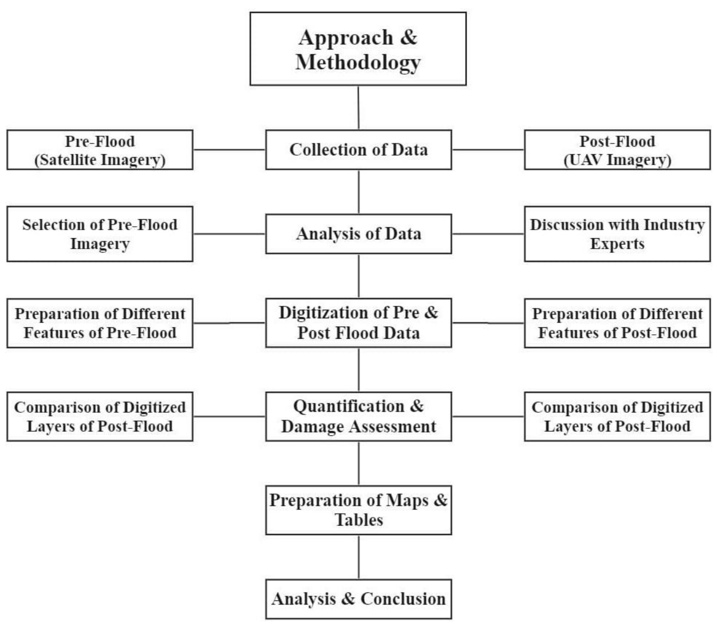

Figure 1. Workflow of UAV data acquisition, image processing, and GIS-based flood assessment applied in the Harnai Khawar study.

Digitization of Ground Features:

Pre- and post-flood datasets were digitized in ArcGIS Pro to identify major landscape elements, including roads, bridges, built-up areas, agricultural fields, retaining walls, active and dry river channels, and community structures such as mosques and water tanks. Manual digitization ensured precision in delineating small structures and enabled a clear and accurate comparison between pre- and post-event conditions. Manual digitization ensured precision for small structures and allowed clear pre- and post-event comparison.

Quantification and Damage Assessment:

The pre- and post-flood datasets were overlaid in ArcGIS Pro to quantify the spatial extent of structural and agricultural damage in Harnai Khawar. Vector layers representing built-up areas, agricultural land, bridges, and retaining walls were compared to calculate changes in area and perimeter. Each feature polygon was examined for displacement, deformation, or inundation relative to its pre-flood footprint.

To standardize the evaluation, all mapped features were classified into three categories based on the degree of physical alteration visible in the post-flood UAV orthomosaics. Fully affected structures included buildings or retaining walls that were destroyed, displaced, or submerged, showing total loss of roof or wall integrity with no remaining usable footprint. Partially affected structures exhibited partial roof collapse, wall breaches, or debris deposition but retained more than half of their original footprint. Minimally affected structures displayed only superficial signs of flooding, such as water marks, sediment accumulation, or slight erosion around the foundation, without significant structural deformation. These classification criteria were established through a detailed side-by-side comparison of pre- and post-flood imagery in *ArcGIS Pro*, ensuring objective differentiation between the varying degrees of impact observed across the study area.

Preliminary Analysis and Interpretation:

Preliminary analysis revealed widespread channel widening, structural wall failures, and significant crop losses across the floodplain. The orthomosaics highlighted extensive damage to retaining walls and the inundation of agricultural terraces along the active Khwar. Agricultural land showed strong reflectance changes due to sediment deposition and erosion. Built-up areas near the channel margins experienced partial or total structural damage.

These patterns confirm that UAV-based data combined with GIS offers rapid, accurate, and spatially detailed evidence of flood impacts, enabling informed planning for reconstruction and risk mitigation.

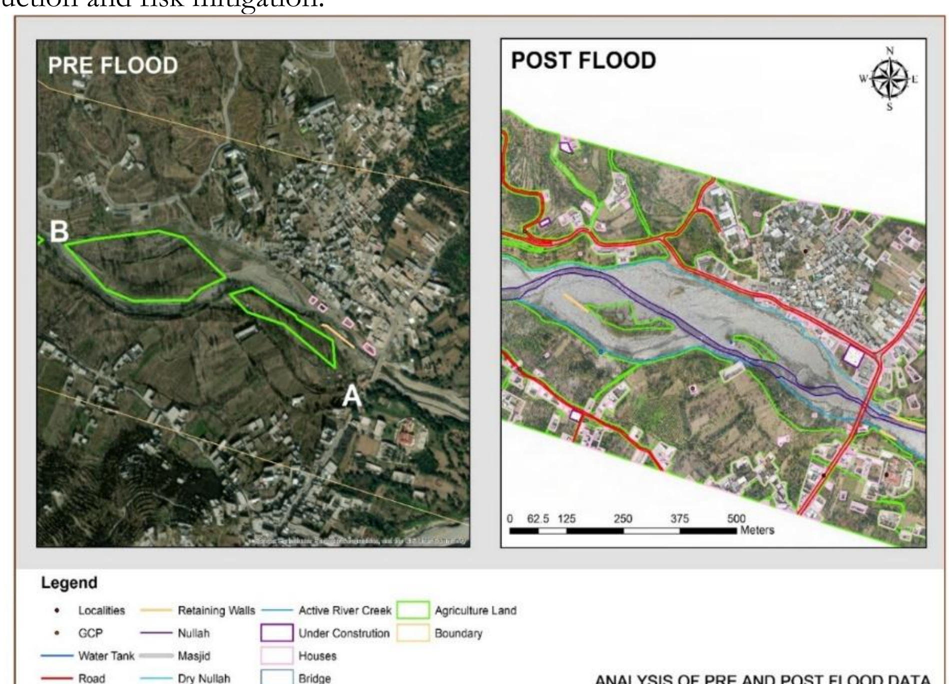

Figure 2. Pre- and post-flood comparison for Barwai Khwar (Swat, KPK). Left: Pre-flood Google Earth imagery (12 June 2022) with agricultural parcels (A–B) outlined in green. Right: Post-flood UAV orthomosaic showing digitized layers, roads (red), retaining walls (orange), active river (dark blue), dry nullah (light blue), bridges, houses (pink), and agricultural boundaries (green), illustrating channel widening and overbank inundation.

Results and Findings:

Overview of Damage Assessment:

The UAV and GIS-based analysis revealed extensive structural and agricultural losses along the Barwai Khwar floodplain. Using orthomosaics and digitized layers, four primary categories of damage were identified: retaining walls, residential structures, agricultural land, and bridges. Each feature was mapped, measured, and tabulated using spatial statistics derived from the pre- and post-flood imagery (Tables 1-4).

Retaining Walls:

Fifteen retaining walls were identified as damaged or destroyed (Table 1). The total measured length of affected walls reached approximately 2,184 m, ranging from 59 m to 283 m per segment. These walls failed primarily at narrow bends and sections where the flood energy concentrated, reflecting hydraulic undercutting and inadequate structural reinforcement.

This observation aligns with studies from mountainous regions where retaining wall collapse is strongly linked with slope instability and high unit stream power. The spatial clustering of failures along outer bends also supports the fluvial geomorphic theory of lateral erosion under peak discharge conditions.

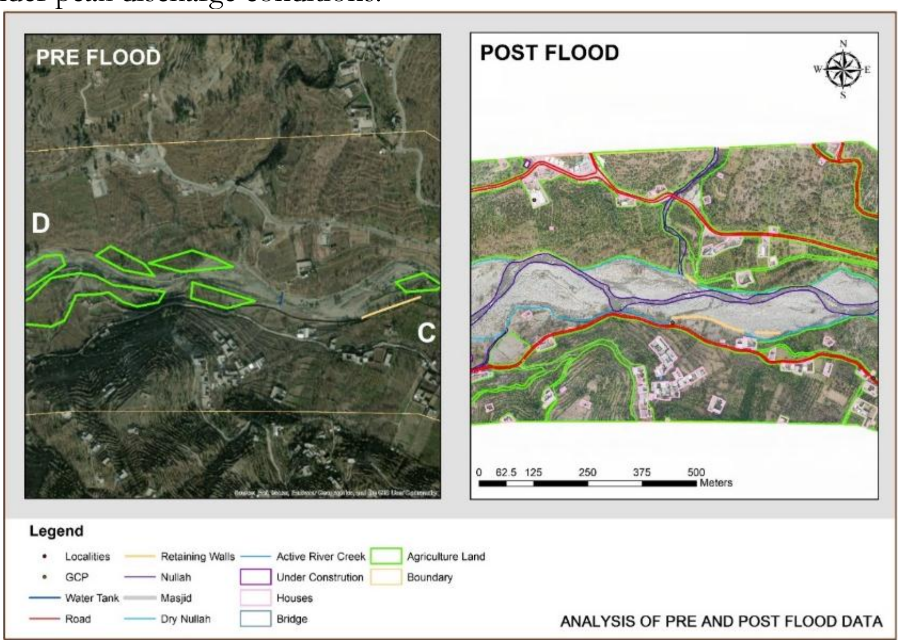

Figure 3. Examples of retaining-wall failures and eroded channel margins captured from UAV orthomosaic after the 2022 flood.

Table 1. Summary of damage length of retaining walls in Barwai Khwar.

Sr. No	Built-up Type	Location (Longitude, Latitude)	Perimeter (m)
1–15	Retaining Walls	72°28'–72°23'E, 35°4'–35°5'N	59–283

Residential Structures:

Thirteen residential structures were mapped as damaged, covering a combined area of 6,271 m² and a total perimeter of 1,075 m (Table 2). The largest destroyed structure (1,438 m²) was located near 35°04'46" N, 72°23'54" E, a low-lying settlement adjacent to the main channel.

These losses mirror findings by [4], who noted that floodplain dwellings near active channels face a disproportionate risk of collapse due to scouring and poor foundation design.

Table 2. Summary of damaged residential structures.

Sr. No	Built-up Type	Location (Longitude, Latitude)	Area (m²)
1–13	Houses	72°23'–72°28'E, 35°4'–35°6'N	87–1,438

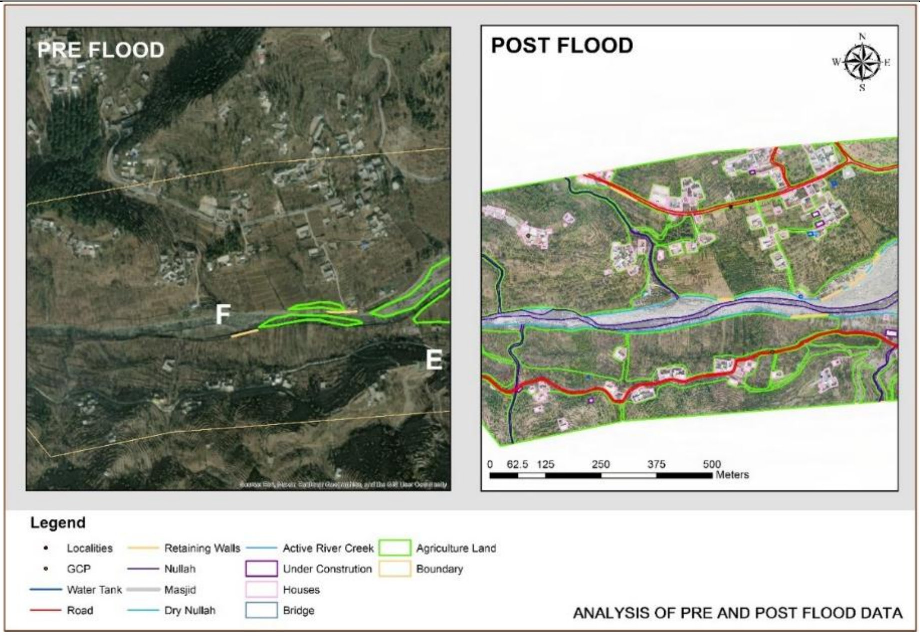

Figure 4. UAV orthomosaic overlay highlighting flood-inundated housing clusters and damaged building footprints in Barwai Khwar.

Agricultural Land:

Agricultural zones suffered the most extensive impact, with 37 parcels affected and a combined damaged area of approximately 22.56 ha (approximately 225,612 m²) (Table 3). Individual plot losses had ranged from 0.1 to 8.5 acres, depending on their proximity to the main channel. The greatest concentration of damage was observed near 35°4'30"N, where floodwaters had deposited thick sediment and destroyed field boundaries. UAV-based observation provided precise parcel-level data, which is critical for estimating compensation and guiding soil rehabilitation.

Table 3. Summary of flood-damaged agricultural land.

Sr. No	Feature	No. of Parcels	Total Area	Perimeter Range
1–37	Agricultural Land	37	22.56 ha	171–866 m

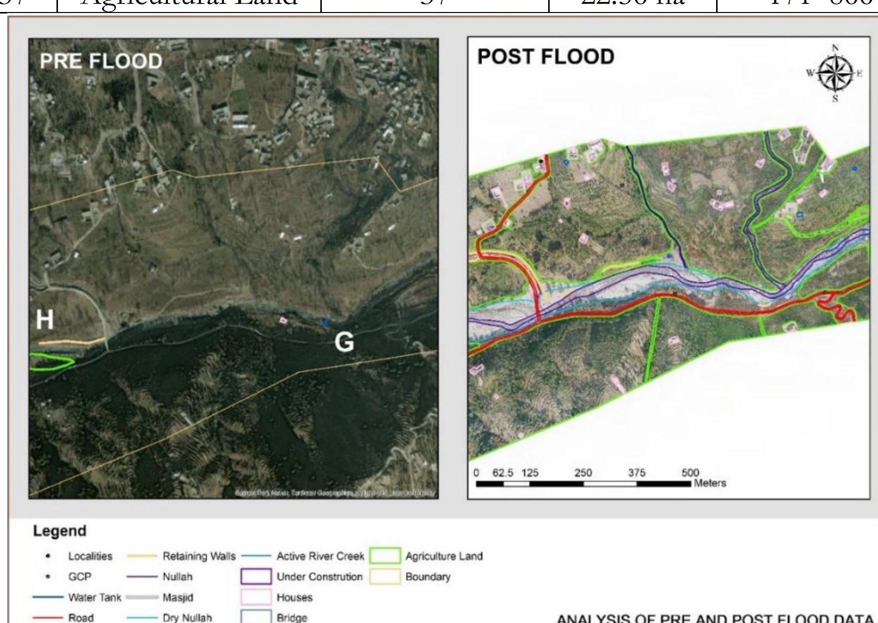

Figure 5. UAV-derived map showing agricultural parcels affected by floodwater inundation and sediment deposition.

Bridges and Linear Infrastructure:

Two bridges suffered severe structural damage, with a total affected length estimated at 39 m (Table 4). The bridge collapse was associated with local scour and heavy debris accumulation at piers, similar to the mechanisms identified by [12]. These localized failures disrupted connectivity between villages and delayed emergency access, emphasizing the need for hydrologically informed bridge design in high-flow mountain basins.

Table 4. Damage length of bridges in Barwai Khwar.

Sr. No	Built-up Type	Location (Longitude, Latitude)	Length (m)
1–2	Bridges	72°27'–72°26'E, 35°4'N	15.4 – 23.6

The total mapped length of the Barwai Khwar nullah was 11,378 m (Figure 6). The active channel width increased from 6.97 m (minimum) to 75.9 m (maximum), representing more than a tenfold expansion at certain locations. This dramatic widening is attributed to lateral erosion and bank collapse under high discharge.

Such fluvial adjustment processes are well-documented in flash-flood environments where unconsolidated alluvial banks fail rapidly. UAV-derived channel metrics thus serve as valuable indicators of hydrodynamic energy and erosion risk.

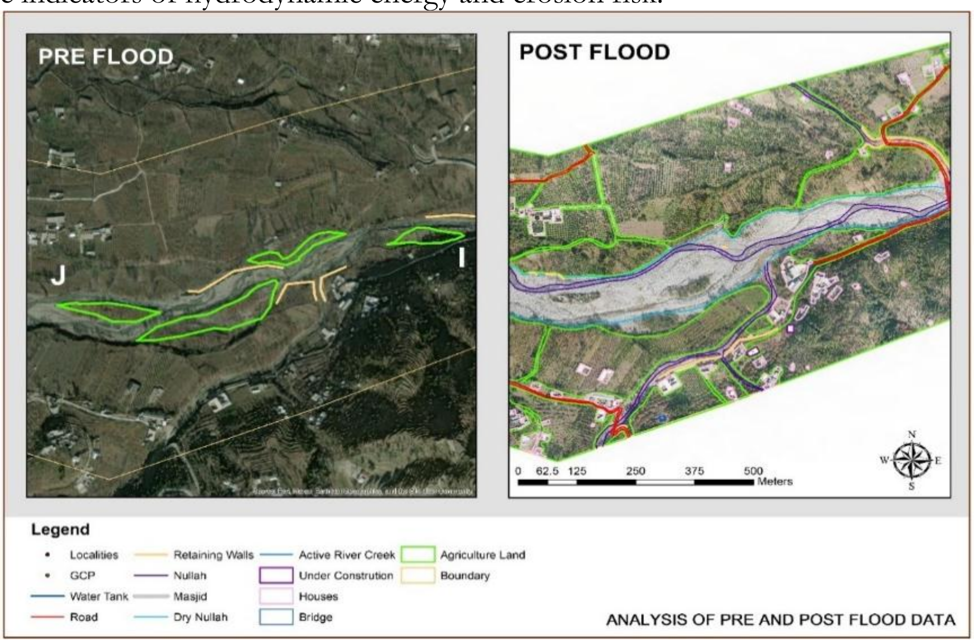

Figure 6. Post-flood UAV imagery showing collapsed bridge deck and bank scour along Barwai Khwar 4.6 Nullah Morphology

Table 5. Variation in the nullah width before and after flood.

Sr. No	Location (Longitude, Latitude)	Width	Remarks
1	72°23'46"E, 35°6'17"N	75.9 m (max)	Severe widening
2	72°25'1"E, 35°4'29"N	6.97 m (min)	Confined reach

Interpretation:

The results demonstrate that the 2022 flood substantially modified both the physical landscape and human infrastructure within Barwai Khwar. The UAV analysis revealed that the active channel width of Harnai Khawar expanded from approximately 7 m to 76 m, accompanied by the collapse of multiple retaining walls and the loss of about 22 ha of agricultural land. These changes occurred primarily along outer bends and high-energy flow zones identified in the post-flood orthomosaic. The integrated UAV–GIS assessment precisely quantified the extent of each damage type, providing measurable indicators of flood impact for recovery and mitigation planning in the study area.

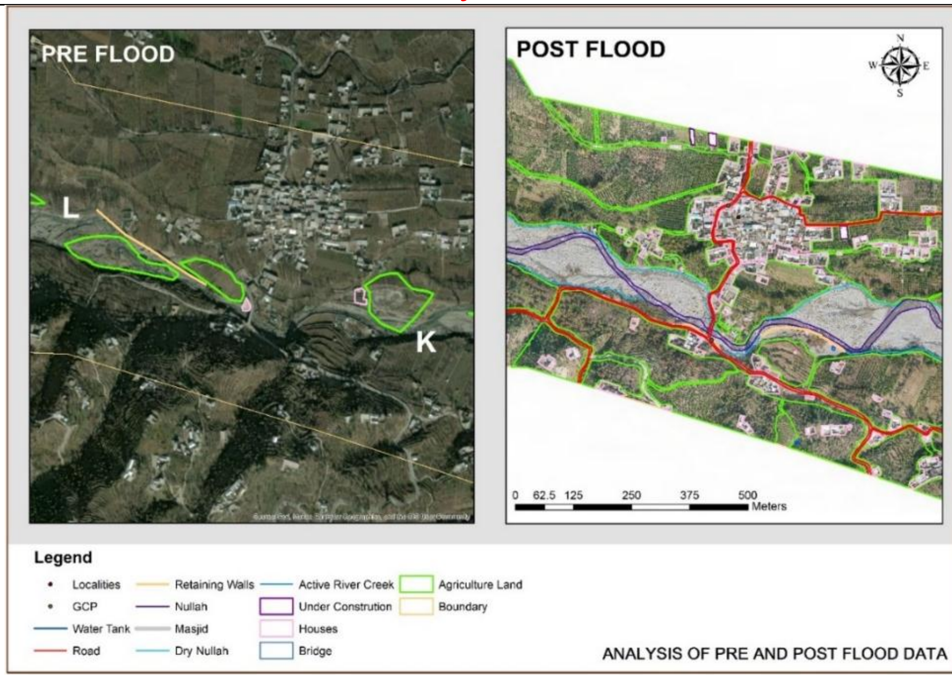

Figure 7. Comparison of pre- and post-flood channel width derived from UAV orthomosaic.

Discussion:

These findings are consistent with agricultural flood studies in other South Asian basins, where sedimentation and erosion jointly reduce land productivity [13]. The UAV-GIS analysis of the 2022 flood in Harnai Khawar revealed substantial geomorphic and infrastructural transformations across the valley, including channel widening, retaining wall failures, and extensive damage to agricultural terraces and built-up zones. The observed increase in channel width from approximately 7 m to nearly 76 m indicates severe lateral erosion driven by high stream power and sediment transport, characteristics typical of flash floods in steep mountain basins of northern Pakistan [3][9]. These findings are consistent with previous studies conducted in similar mountainous environments. Elkhrachy [14] identified the same mechanisms of slope instability and hydraulic undercutting as major contributors to retaining wall failures in Najran City, Saudi Arabia. Likewise, Voogt and White [12] documented concentrated damage along outer meander bends during the 2013 Alberta floods, demonstrating that localized energy gradients amplify geomorphic instability. The similarity between these outcomes and those observed in Harnai Khawar underscores that steep gradients and unreinforced slopes remain critical determinants of structural vulnerability.

The loss of agricultural land, estimated at approximately 22 ha, is comparable to findings from other South Asian floodplains, where sediment deposition and topsoil removal have been shown to degrade agricultural productivity [13]. Long et al. used synthetic aperture radar (SAR) data to map flood extents in Namibia and similarly concluded that sediment accumulation and erosion jointly diminish soil fertility. The parcel-level detail achievable through UAV-based mapping in this study, however, offers finer spatial accuracy than conventional satellite-based approaches, enabling more precise quantification of crop losses for rehabilitation planning. Structural damage to bridges and transport infrastructure observed in Harnai Khawar also aligns with earlier research. Emphasized that debris accumulation at bridge piers is a major factor leading to collapse under high discharge, consistent with the localized failures recorded during this event. Demonstrated through UAV mapping after Hurricane Matthew that bridge scour and abutment erosion are direct outcomes of concentrated hydraulic pressure, a condition similarly detected in this valley. The application of UAV-derived orthomosaics and photogrammetry demonstrated higher spatial fidelity than satellite or field surveys commonly used in Pakistani studies [1][9]. While past research primarily focused on large-scale basin analyses such as the Indus or Chenab, the present work introduces a scalable, high-resolution workflow for smaller tributaries where topographic complexity limits traditional assessment techniques. Comparable advances have been reported by Hashemi-Beni et al. [7] and Zawadzka et al. [6], who both demonstrated that UAV-based digital elevation models and object-oriented classifications yield centimeter-scale insights critical for urban and fluvial flood assessments.

Furthermore, this study extends the regional understanding of monsoon-driven geomorphology in the Hindu Kush, Karakoram, and Himalayan (HKH) domain. Recent work by Bazai et al. [10] and Khan et al. [11] emphasized the intensification of hydrometeorological hazards in Swat due to increased rainfall variability and deforestation. The spatial evidence from Harnai Khawar corroborates their observations, illustrating that unregulated slope modification and encroachment onto floodplains exacerbate the destructive potential of extreme rainfall events. Overall, the results validate that UAV-based photogrammetry integrated with GIS analytics provides a reliable, rapid, and cost-effective solution for post-flood damage assessment. It complements regional hydrological and hazard models by adding detailed spatial data essential for localized risk management. The workflow presented here bridges the gap between large-scale remote sensing studies and on-ground disaster assessment, contributing to Pakistan's growing need for operational geospatial solutions in mountainous terrains.

Conclusion:

The 2022 flood in Harnai Khawar, Swat, caused major geomorphic and infrastructural transformations across the valley. UAV and GIS analysis showed widespread losses in agricultural land, retaining walls, residential buildings, and linear infrastructure. The river channel widened from about 7 m to nearly 76 m in several reaches, eroding terraces and destroying flood-protection structures. Agricultural land suffered the highest impact, followed by housing clusters near the river margins and retaining walls along outer bends. Two bridges were completely damaged, cutting off access between nearby settlements. These observations highlight how strong monsoon flows can quickly reshape valley morphology and threaten livelihoods in steep basins such as Swat.

The study confirms the effectiveness of UAV-based remote sensing for rapid, precise, and low-cost flood assessment in mountainous regions. High-resolution imagery provided fine-scale evidence of flood impacts and supported accurate mapping of damaged assets. The integrated UAV-GIS workflow demonstrated here can serve as a replicable framework for disaster monitoring, risk evaluation, and reconstruction planning in other flood-prone areas of Pakistan.

Recommendations:

Rapid recovery and rehabilitation efforts should be prioritized to rebuild damaged bridges, retaining walls, and road networks in order to restore connectivity and stability for the affected communities. Strengthening flood resilience requires the use of flood-resistant construction materials, improved drainage systems, and slope protection measures, while afforestation and vegetative buffers can effectively reduce surface runoff and soil erosion. Establishing community-based early warning systems, conducting regular drills, and maintaining efficient communication networks are essential for minimizing losses during extreme flood events. Sustainable land-use planning must also be adopted to restrict construction within active floodplains and to promote agricultural practices that adapt to evolving hydrological conditions. In parallel, public awareness and capacity-building programs should be implemented to educate residents on flood preparedness, empowering them to take preventive measures and respond effectively to future disasters. Finally, collaborative governance between local authorities, provincial institutions, and NGOs is crucial for ensuring coordinated flood management, informed decision-making, and sustainable recovery across the region.

Acknowledgments:

The authors acknowledge the European Space Agency (ESA) for providing GLO-DEM data and thank the local authorities of the Swat District for their cooperation during UAV surveys in the Harnai Khawar area.

Author's Contribution:

I.H. designed the study, performed UAV data analysis, and prepared the original manuscript draft. R.Q. assisted in methodology development and GIS processing. A. A contributed to data interpretation, map preparation, and validation of results. M.S. contributed to data interpretation, write-up, and formatting. S.U.A. supervised the research, reviewed the manuscript, and guided the analytical workflow.

Conflict of Interest: The Authors declare that there is no conflict of interest in publishing this manuscript in IJIST.

References:

[1] S. A. Ahmed, K., Ullah, S., & Khan, "Event Analysis: 2022 Floods in Swat Valley, Pakistan," *Reliefweb*, 2023, [Online]. Available: https://reliefweb.int/report/pakistan/event-analysis-2022-floods-swat-valley-pakistan

[2] M. Aslam, "Flood Management Current State, Challenges and Prospects in Pakistan: A Review," *Mehran Univ. Res. J. Eng. Technol.*, vol. 37, no. 2, 2018, [Online]. Available: https://publications.muet.edu.pk/index.php/muetrj/article/view/199

[3] N. A. Bazai *et al.*, "Dynamics and impacts of monsoon-induced geological hazards: A 2022 flood study along the Swat River in Pakistan," *Nat. Hazards Earth Syst. Sci.*, vol. 25, no. 3, pp. 1071–1093, Mar. 2025, doi: 10.5194/NHESS-25-1071-2025.

[4] K. Calvin *et al.*, "IPCC, 2023: Climate Change 2023: Synthesis Report. Contribution of Working Groups I, II and III to the Sixth Assessment Report of the Intergovernmental Panel on Climate Change [Core Writing Team, H. Lee and J. Romero (eds.)]. IPCC, Geneva, Switzerland.," Jul. 2023, doi: 10.59327/IPCC/AR6-9789291691647.

[5] I. Elkhrachy, "Flash Flood Hazard Mapping Using Satellite Images and GIS Tools: A case study of Najran City, Kingdom of Saudi Arabia (KSA)," *Egypt. J. Remote Sens. Sp. Sci.*, vol. 18, no. 2, pp. 261–278, 2015, doi: https://doi.org/10.1016/j.ejrs.2015.06.007.

[6] L. Hashemi-Beni, J. Jones, G. Thompson, C. Johnson, and A. Gebrehiwot, "Challenges and Opportunities for UAV-Based Digital Elevation Model Generation for Flood-Risk Management: A Case of Princeville, North Carolina," *Sensors*, vol. 18, no. 11, p. 3843, 2018, doi: https://doi.org/10.3390/s18113843.

[7] N. A. Khan *et al.*, "Flood risk assessment in the Swat river catchment through GIS-based multi-criteria decision analysis," *Front. Environ. Sci*, vol. 13, 2025, doi: https://doi.org/10.3389/fenvs.2025.1567796.

[8] K. R. Krishna, "Agricultural Drones A Peaceful Pursuit," *Routledge*, 2018, [Online]. Available: https://www.routledge.com/Agricultural-Drones-A-Peaceful-Pursuit/Krishna/p/book/9781774636428?srsltid=AfmBOorg0c8AHJ21NhBoPiSUB-4cmcdx-0FifTWhsHqC1qQ42yP-u1QA

[9] Y. L. Wenning Li, "Urban Water Extraction with UAV High-Resolution Remote Sensing Data Based on an Improved U-Net Model," *Remote Sens*, vol. 13, no. 16, p. 3165, 2021, doi: https://doi.org/10.3390/rs13163165.

[10] T. E. F. and F. P. Stephanie Long, "Flood extent mapping for Namibia using change detection and thresholding with SAR," *Environ. Res. Lett.*, vol. 9, no. 3, 2014, doi: 10.1088/1748-9326/9/3/035002.

[11] H. A. & N. K. Sadia Mariam Malik, "Mapping vulnerability to climate change and its repercussions on human health in Pakistan," *Global. Health*, vol. 8, 2012, doi:

https://doi.org/10.1186/1744-8603-8-31.
[12] J. Zawadzka, I. Truckell, A. Khouakhi, and M. Rivas Casado, "Detection of Flood Damage in Urban Residential Areas Using Object-Oriented UAV Image Analysis Coupled with Tree-Based Classifiers," *Remote Sens.*, vol. 13, no. 19, p. 3913, 2021, doi: https://doi.org/10.3390/rs13193913.
[13] S. Zakaria, M. R. Mahadi, A. F. Abdullah, and K. Abdan, "Aerial Platform Reliability for Flood Monitoring Under Various Weather Conditions: A Review," *Lect. Notes Geoinf. Cartogr.*, pp. 295–314, 2019, doi: 10.1007/978-3-030-05330-7_12.
[14] L. Wouters, A. Couasnon, M. C. De Ruiter, M. J. C. Van Den Homberg, A. Teklesadik, and H. De Moel, "Improving flood damage assessments in data-scarce areas by retrieval of building characteristics through UAV image segmentation and machine learning - A case study of the 2019 floods in southern Malawi," *Nat. Hazards Earth Syst. Sci.*, vol. 21, no. 10, pp. 3199–3218, Oct. 2021, doi: 10.5194/NHESS-21-3199-2021.